ISBN: 978-3-95450-227-1 ISSN: 2673-5490 doi:10.18429/JACoW-IPAC2022-WEOZSP1

LONGITUDINAL BUNCH SHAPING USING AN X-BAND TRANSVERSE DEFLECTING CAVITY POWERED BY WAKEFIELD POWER EXTRACTOR AT ARGONNE WAKEFIELD ACCELERATOR FACILITY*

Seong-Yeol Kim†, John Power, Gongxiaohui Chen, Scott Doran, Wanming Liu, Eric Wisniewski
Argonne National Laboratory, Lemont, IL 60439, USA
Chunguang Jing‡, Alexis Bibian, Ernest William Knight, Sergey Kuzikov
Euclid Techlabs, Bolingbrook, IL 60440, USA
Philippe Piot, Northern Illinois University, DeKalb, IL 60115, USA

Abstract

Longitudinal bunch shaping using transverse deflecting cavities (TDC) was recently proposed [Gwanghui Ha *et al., Phys. Rev. Accel. Beams* **23**, 072803, 2020]. This configuration is well suited for shaping the current profile of high-charge bunches since it does not use dipole magnets, and therefore, is not prone to deleterious effects arising from coherent synchrotron radiation. An intercepting mask located downstream of the first TDC, which introduce a spatiotemporal correlation, transversely shape the beam. Downstream of the second TDC, upon removal of the cross-plane correlation, the bunch is temporally shaped. In this paper, we investigate longitudinal bunch shaping with an X-band TDC powered by an X-band, short-pulse wakefield Power Extraction and Transfer Structure (PETS), where the wakefield from the drive beam propagating through the PETS is the power source. We describe the RF designs of the X-band TDC and the configuration of the overall shaping system. Finally, we explore via beam-dynamics simulations the performances of the proposed shaper and its possible application to various bunch shapes relevant to beam-driven acceleration and coherent radiation generation.

INTRODUCTION

Longitudinal bunch shaping demonstration has been actively investigated to achieve high-gradient accelerating field through structure or plasma-based accelerators and to improve the acceleration efficiency of the witness beam through those advanced accelerators. In particular, experimental demonstrations have been carried out to generate the electron beam where the longitudinal distribution is triangle, thus being used as a drive source in the wakefield accelerator, increasing the transformer ratio of the wakefield to be larger than 2 [1–3]. In order to increase the transformer ratio and high-gradient at the same time, drive beam charge should be increased further given that the beam energy is fixed [4].

For the manipulation of high-charge beam, we can consider well-developed beam manipulation techniques such as emittance exchange beamline [5–7], shaping of the laser [8], and energy-correlation-based shaping method [9–11]. However, those methods have limitations for the high-charge beam manipulation due to i) coherent synchrotron radiation (CSR) and ii) space charge force.

To overcome the limitations on the beam manipulation with high-charge beam, use of transverse-deflecting cavity (TDC) arises an alternative solution [12–15]. The TDC-based beamline is straight line; we do not need to consider the effects of the CSR. In addition, this shaping method is used where the beam to be shaped is relativistic. Therefore, we do not significantly consider the space charge effects.

In this paper, we will show the X-band TDC powered by Power Extractor and Transfer Structure (PETS) installed at the Argonne Wakefield Accelerator (AWA) facility. X-band TDC-based longitudinal bunch shaping system will also be shown. In addition, the bunch shaping results with mask, obtained by the particle tracking results, will be presented.

TDC-BASED SHAPING SYSTEM

A schematic view of the TDC-based shaping system is shown in Fig. 1. Note that this shaping method is based on

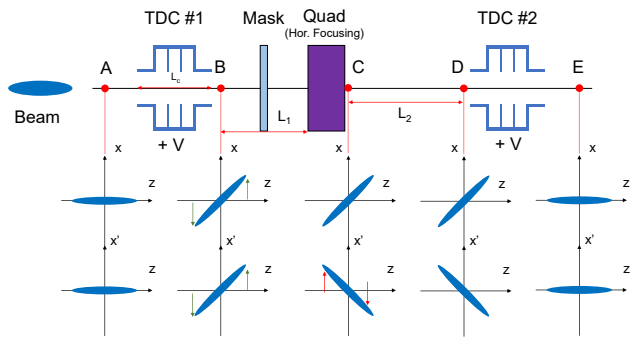

Figure 1: Schematic vewi of the TDC shaping system. Beam propagates from left to right. At different positions from A to E, electron beam phase spaces are shown.

preceding studies reported in Refs [12, 15]. It consists of two TDCs. In between TDCs, mask and quadrupole magnet are installed. From the position A to E, slice distribution $(z - x)$ and $(z - x')$ are shown. From A, as the beam propagates through the TDC, the beam is kicked in longitudinal plane, and z-slice information is projected into $(x - y)$ plane. Then, using the mask, the longitudinal distribution is tailored. The quadrupole magnet installed inside the system is to rotate the horizontal divergence, changing the angle of $(z - x')$

* Work supported by DoE SBIR Grant DE-SC0021733
† seongyeol.kim@anl.gov
‡ jingchg@anl.gov

ISBN: 978-3-95450-227-1 ISSN: 2673-5490 doi:10.18429/JACoW-IPAC2022-WEOZSP1

phase space. Since the beam is still tilted, this transverse-longitudinal correlation should be removed. This removal can be performed by using the second TDC.

In order to perfectly remove the correlations $(z - x)$ and $(z - x')$, one should moderately choose the strength of the TDC kick and quadrupole magnet with given drift spaces. Using the first-order transfer matrix of TDC and thin lens approximation of the quadrupole magnet, the condition can be obtained, as shown in Eqs. (1–2) [15].

$$f_1 = \frac{\left(L_1 + \frac{L_c}{2}\right)\left(L_2 + \frac{L_c}{2}\right)}{L_1 + L_2 + L_c}, \tag{1}$$

$$\kappa_2 = \frac{2L_1 + L_c}{2L_2 + L_c}\kappa_1, \tag{2}$$

where f_1 is the focal length of the quadrupole magnet, $L_{1,2}$ are the drift spaces, L_c is TDC length shown in Fig. 1, and $\kappa_{1,2}$ are the TDC kick strength $\left(\kappa = \frac{eV_\perp}{pc}\frac{2\pi}{\lambda}\right)$. λ is RF wavelength. If Eqs. (1–2) are satisfied, then the transverse-longitudinal correlations after the system become zero.

X-BAND TDC

We will mainly have discussions with X-band TDC where the operational frequency is 11.7 GHz. The advantage of using X-band TDC at the AWA facility is following: A Power Extractor and Transfer Structure (PETS) [16] is installed in the facility, which creates up to 400 MW RF power [17, 18] by using 60 MeV, 450 nC drive electron bunch train. In addition, since the pulse length from the PETS is about 10 ps, it is expected that the breakdown limit is improved by using the short pulse. Therefore, length of the TDC can be kept small, while the kick strength κ can remain very large, leading to the reduction on the overall length of the shaping system.

Figure 2 shows the X-band TDC structure. It consists of two independent cells, and the power is fed by means of 3-dB coupler. Operational frequency is 11.7 GHz, and fundamental mode is TE11 mode. Therefore, the deflecting and streaking of the beam is mainly performed with the transverse time-dependent electric field. In order to make a phase difference in between two cells to be $\pi/2$, which is a fundamental property of 3-dB coupler, the spacing between two cells should satisfy the condition $L = \frac{\lambda}{4} + n\lambda$ where n is integer. In our design, L is chosen to be approximately 19.2 mm.

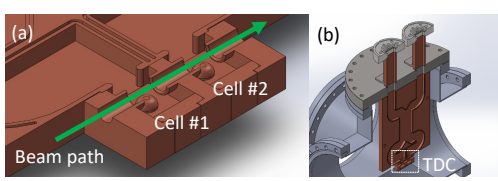

Figure 2: X-band TDC structure. (a) cut view of the structure. (b) cut view of the structure installed inside the vacuum chamber.

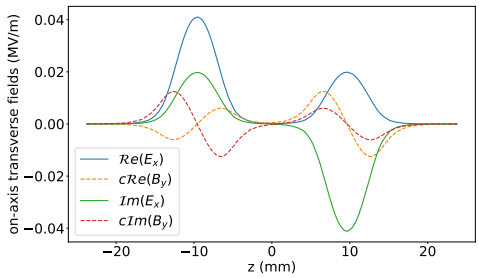

Figure 3: X-band TDC structure. (a) cut view of the structure. (b) cut view installed in the vacuum chamber.

Table 1: The AWA Drive Beam Parameters

Parameter	Value
Energy, E	60.00 MeV
Energy spread, σ_δ	1.79%
Charge, Q	40.00 nC
Initial FWHM UV length, σ_t	3.00 ps

EM field of the TDC can be seen in Fig 3. An incident power to the TDC is 1 W, and the peak E_x field gradient is found to be around 41 kV/m; when the incident power to the TDC becomes 100 MW, then the peak E_x field gradient will be around 410 MV/m.

SHAPING SYSTEM CONFIGURATION AND START-TO-END SIMULATION RESULTS

In this study, start-to-end simulations have been performed with the OPAL simulation code [19], which supports 3D space charge force calculation.

RMS beam envelope along the TDC shaping system is illustrated in Fig. 4. Input of the electron beam is obtained by the tracking simulation of the drive linac section including four quadrupole magnets downstream of the linac section. The initial beam parameters are shown in Table 1; The initial beam envelope at the beginning of the system was optimized by using the DEAP Python module [20] for Multi-Objective Genetic Algorithm (MOGA) together with the OPAL simulation.

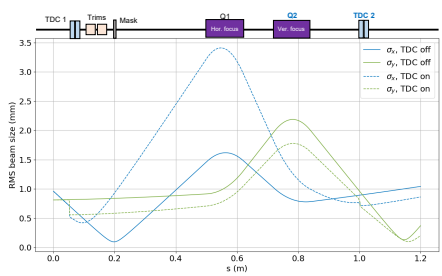

Figure 4: RMS beam size along the TDC-based shaping system.

ISBN: 978-3-95450-227-1 ISSN: 2673-5490 doi:10.18429/JACoW-IPAC2022-WEOZSP1

In this shaping system, there are two constraints; i) 5.0 mm diameter of TDC aperture, and ii) 25 mm of beam pipe diameter. Since the aperture size of the TDC is very small, RMS beam size along the TDC should be less than 1.0 mm. In addition, additional quadrupole magnet is installed to control the vertical beam size matched with the aperture size of the second TDC. In particular, position and strength of the quadrupole magnets, and the strength of second TDC were moderately chosen to satisfy all the constraints as well as the shaping condition. Optimized parameters are listed in Table 2. Finally, it is worth noting that the entire length of the shaping system is around 1.0 m.

We mainly discuss the bunch shaping for triangular distribution. The final shaped beam and its comparison with the initial slice distribution before the TDC-based shaping system are also shown in Fig. 5. The longitudinal density

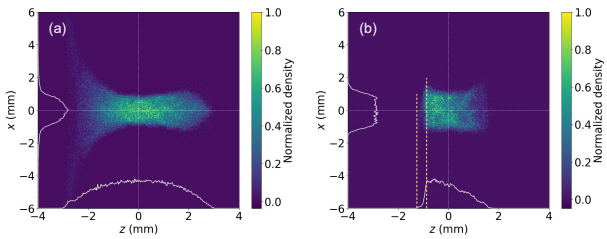

Figure 5: $(x-y)$ distribution (a) at the entrance of the shaping system and (b) after the shaping system. Head is at positive z, whereas the tail at negative z.

distribution becomes the triangular shape. Beam charge after the system is 12.63 nC, and total bunch length becomes 9.43 ps in time. Since the final task through this bunch shaping is to demonstrate the high-transformer, high-gradient wakefield generation through the dielectric structure, the target parameters are i) beam charge of larger than 10 nC and ii) total bunch length of less than 10 ps. Therefore, the obtained beam parameters satisfy the target parameters.

In terms of the shaping quality, as marked with yellow dashed lines in Fig. 5(b), there is short ramp region at the beam tail. From the peak to the zero density, its length is about 0.4 ps in time. This is mainly due to the horizontal beam parameters such as RMS beam size and emittance at the mask. The $(z-x)$ slice distributions along the mask position are described in Fig. 6. At the mask position, the

Table 2: Optimized TDC Shaping System Parameters

Parameter	Value
TDC1 $E_{x,peak}$	75.00 MV/m
TDC2 $E_{x,peak}$	35.32 MV/m
Q1 strength k_1	10.000 T/m
Q2 strength k_2	-10.314 T/m
Quadrupole magnet length	0.12 m
Drift from TDC1 end to Q1 front	0.412 m
Drift from Q1 end to Q2 front	0.100 m
Drift from Q2 end to TDC2 front	0.160 m

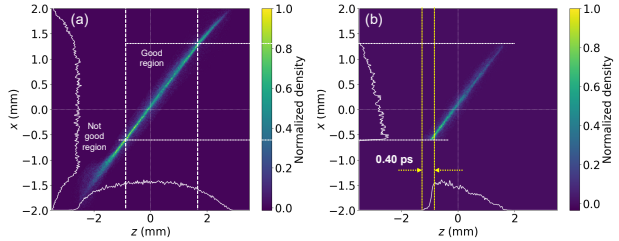

Figure 6: $(z-x)$ distribution (a) before the mask and (b) after the mask.

horizontal beam size is minimized as shown in Fig. 4 where there is no TDC. Fig. 6(a) shows the distribution right before the mask position where the TDC is turned on. Therefore, we can find the horizontal beam distribution along the slice where the beam is tilted by the TDC. Around the core of the slice, however, there are some halo particles. It is mainly due to the second-order aberrations around the drift-quadrupole section. The particles placed in "not good region" Fig. 6(a) have larger and mismatched slice phase space compared to that in "good" region. When the beam is cut by the mask, the halo particles build up the degradation of the shaping quality as shown in Fig. 6(b), and that build-up by the horizontal beam size in addition to the emittance [15] affects the final shaping quality. Therefore, to improve the shaping quality, horizontal beam size and emittane should be minimized, and the slice horizontal phase space should be aligned along the longitudinal slice.

CONCLUSION

We verified that the longitudinal bunch shaping with X-band TDC powered by the PETS is feasible; beam charge after the TDC-based shaping system is about 12.63 nC, and total bunch length is 9.43 ps in time, which satisfy the target parameters for structure wakefield experiments. As a future work, we will discuss the shaping for other distributions such as doorstep and bunch train distributions. In addition, using the pre-shaped UV pulse, we will investigate the improvement of the charge capturing efficiency of the TDC-shaping system.

ACKNOWLEDGEMENTS

Authors thank Tianzhe Xu for his valuable comments for optimization of the drive linac and mask shapes. This work was supported by DoE SBIR Grant DE-SC0021733 and by the U.S. Department of Energy (DOE), Office of Science, under contract No. DE-AC02-06CH11357 with Argonne National Laboratory (ANL). The computing resources used for this research were provided on BEBOP, a high-performance computing cluster operated by the Laboratory Computing Resource Center (LCRC) at ANL.

ISBN: 978-3-95450-227-1 ISSN: 2673-5490 doi:10.18429/JACoW-IPAC2022-WEOZSP1

REFERENCES

[1] Q. Gao *et al.*, "Observation of high transformer ratio of shaped bunch generated by an emittance-exchange beam line", *Phys. Rev. Lett.*, vol. 120, p. 114801, Mar. 2018.

[2] R. Roussel *et al.*, "Single shot characterization of high transformer ratio wakefields in nonlinear plasma acceleration", *Phys. Rev. Lett.*, vol. 124, p. 044802, Jan. 2020.

[3] G. Loisch *et al.*, "Observation of high transformer ratio plasma wakefield acceleration", *Phys. Rev. Lett.*, vol. 121, p. 064801, Aug. 2018.

[4] S. S. Baturin and A. Zholents, "Upper limit for the accelerating gradient in the collinear wakefield accelerator as a function of the transformer ratio", *Phys. Rev. Accel. Beams*, vol. 20, p. 061302, Jun. 2017.

[5] M. Cornacchia and P. Emma, "Transverse to longitudinal emittance exchange", *Phys. Rev. ST Accel. Beams*, vol. 5, p. 084001, Aug. 2002.

[6] P. Piot, Y.-E. Sun, J. G. Power, and M. Rihaoui, "Generation of relativistic electron bunches with arbitrary current distribution via transverse-to-longitudinal phase space exchange", *Phys. Rev. ST Accel. Beams*, vol. 14, p. 022801, Feb. 2011.

[7] G. Ha *et al.*, "Precision control of the electron longitudinal bunch shape using an emittance-exchange beam line", *Phys. Rev. Lett.*, vol. 118, p. 104801, Mar. 2017.

[8] G. Loisch *et al.*, "Photocathode laser based bunch shaping for high transformer ratio plasma wakefield acceleration", *Nucl. Instrum. Methods Phys. Res. Sect. A*,vol. 909, pp. 107–110, 2018.

[9] P. Muggli, V. Yakimenko, M. Babzien, E. Kallos, and K. P. Kusche, "Generation of trains of electron microbunches with adjustable subpicosecond spacing", *Phys. Rev. Lett.*, vol. 101, p. 054801, Jul. 2008.

[10] P. Muggli *et al.*, "Simple method for generating adjustable trains of picosecond electron bunches", *Phys. Rev. ST Accel. Beams*, vol. 13, p. 052803, May 2010.

[11] C. A. Lindstrøm *et al.*, "Energy-spread preservation and high efficiency in a plasma-wakefield accelerator", *Phys. Rev.Lett.,* vol. 126, p. 014801, Jan. 2021.

[12] E. Kur, G. Penn, J. Qiang, M. Venturini, R. Wells, and A. Zholents, "Accelerator design study for a soft x-ray free electron laser at the lawrence berkeley national laboratory", Tech. Rep. No. LBNL-2670E, 2009.

[13] J. Qiu, G. Ha, C. Jing, S. V. Baryshev, B. W. Reed, J. W. Lau, and Y. Zhu, "Ghz laser-free time-resolved transmission electron microscopy: A stroboscopic high-duty-cycle method", *Ultramicroscopy*, vol. 161, pp. 130–136, 2016.

[14] Y.-C. Du, W.-H. Huang, and C.-X. Tang, "A new method to generate relativistic comb bunches with tunable subpicosecond spacing", *Chinese Physics C*, vol. 36, pp. 151–155, Feb. 2012.

[15] G. Ha, J. G. Power, J. Shao, M. Conde, and C. Jing, "Coherent synchrotron radiation free longitudinal bunch shaping using transverse deflecting cavities", *Phys. Rev. Accel. Beams*, vol. 23, p. 072803, Jul. 2020.

[16] C. Jing *et al.*, "Electron acceleration through two successive electron beam driven wakefield acceleration stages", *Nucl. Instrum. Methods in Phys. Res. Sect. A*, vol. 898, pp. 72–76, 2018.

[17] J. Shao *et al.*, "Generation of high power short Rf pulses using an x-band metallic power extractor driven by high charge multi-bunch train", in *Proc. 10th Int. Particle Accelerator Conf. (IPAC'19)*, Melbourne, Australia, May 2019, pp. 734–737. doi:10.18429/JACoW-IPAC2019-MOPRB069

[18] J. Power, "Private communication."

[19] A. Adelmann *et al.*, "OPAL a versatile tool for charged particle accelerator simulations", May 2019. doi:10.48550/arxiv.1905.06654

[20] F.-A. Fortin, F.-M. De Rainville, M.-A. Gardner, M.Parizeau, and C. Gagné, "DEAP: Evolutionary algorithms made easy", *J. Mach. Learn. Res.,* vol. 13, pp. 2171–2175, Jul. 2012.